



Sustainable Solutions for Energy and Environment, EENVIRO - YRC 2015, 18-20 November
2015, Bucharest, Romania

Measurement of Wind Flow Behavior at the Leeward Side of Porous Fences Using Ultrasonic Anemometer Device

Mohamad Mustafa^a, Yizhong Xu^a, Geogre Haritos^b, Kosugi Kenji^c

^a*Narvik University College, Narvik, Norway* *

^b*University of Hertfordshire, Hatfield, UK*

^c*Shinjo Cryospheric Environment Laboratory, Shinjo, Japan*

Abstract

Efficiency of wind fences is evaluated by the reduction of wind velocity and the effective shelter area behind the fence. Fence porosity is the most influential structural parameters in the porous fence design, and has significant impact on the structure of wind velocity and turbulence leeward. In this work, three fences with porosity of 23%, 35% and 45% have been tested under 10m/s inlet velocity in an environmental wind tunnel. An ultrasonic anemometer was used to measure three dimensional velocity vectors and the fluctuations of velocity vectors with a designed spatial resolution. The obtained data were used to calculate velocity magnitudes, turbulence intensities and turbulent kinetic energies in the test domain. Porosity influencing the structure of turbulence intensity and effective fence zone were discussed in this paper. Neither the distribution of wind velocities nor the structure of turbulence alone can provide sufficient information to assess the performance of porous fences. Consideration of the targeted reduction rate of wind velocity needs to be taken for optimal fence design.

© 2016 The Authors. Published by Elsevier Ltd. This is an open access article under the CC BY-NC-ND license

(<http://creativecommons.org/licenses/by-nc-nd/4.0/>).

Peer-review under responsibility of the organizing committee EENVIRO 2015

Keywords: Ultrasonic anemometry; windbreak; porosity; sheltered zone; wind velocity

1. Introduction

In wintry cold regions like Norway and offshore oil structures in the North Sea, outdoor environment can be extremely hostile and unsustainable for human activities. In order to moderate such climate of the working environment, it is necessary to redirect wind and reduce wind velocity in a confined space. This can be achieved by

* Corresponding author.

E-mail address: MohamadYazidF.Mustafa@hin.no

using windbreaks, which can be rows of trees, structures or artificial shields such as fences. Reduction in wind velocity at the leeward side of the fence modifies the environment in the sheltered zone. Porous fence is one of the artificial devices widely used as windbreaks to mitigate the damages caused by strong wind and transported sediments effectively. It is usually constructed to have optical porosities greater than zero in order to produce artificial windbreaks and block sediment intrusions.

Nomenclature

β	porosity of fence
β_{crit}	critical porosity of fence
h	measuring height
H	fence height
x	horizontal distance from fence
PMT	Point-Measuring Technique
WFMT	Whole-Field Measuring Technique
PIV	Particle-Image Velocimetry
PTV	Particle-Tracking Velocimetry
HWA	Hot-Wire anemometer
PWA	Pulsed-Wire anemometer
LDA	Laser-Doppler anemometer
PDA	Phase-Doppler anemometer
UA	Ultrasonic anemometer

The blowing wind against the windbreak causes air pressure to build up on the windward side, which forces air to move towards the top of the fence and around the sides. Porosity is the ratio of the open area of the windbreak to the total area, and it is one of the most influential structural factors to determine the effectiveness of fences.

Wind flows through the open portions of a windbreak; this flow is termed as the bleed flow, thus the lower the porosity of the barrier, the less bleed flow will occur. Low pressure develops on the leeward side of windbreaks with less porosity. This low-pressure area behind the windbreak causes air to move over the windbreak downward, creating turbulence and reducing protection downwind. As porosity increases, the amount of bleed flow passing through the pores of the windbreak increases, moderating the low pressure and turbulence and increasing the downwind-protected area. While this protected area is larger, the wind speed reductions are not as great. By adjusting windbreak porosity, different wind flow patterns and areas of protection are established. The structure of airflow behind a porous fence is complex due to the presence of the bleed flow passing through the pores in the fence and the displaced flow passing over the fence. Fig.1. shows a comparison of flow regimes behind porous fences for porosities above and under critical porosity, where β is porosity of fence, and β_{crit} is critical porosity of fence [1, 3].

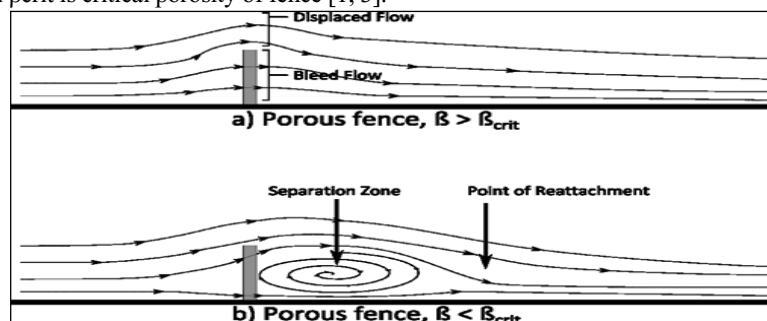


Fig. 1: Comparison of flow regimes behind porous fences as porosity approaches critical porosity [1]

Critical porosity, β_{crit} is defined as the maximum fence porosity below which flow separation and reversal occurs [3]. Above the critical porosity, the airflow in the leeward is dominant by bleed flow and there is no flow separation; (Fig.1, a).

Below critical porosity, the leeward airflow directly behind the fence reverses, resulting in a region of recirculating air (Figure1, b). In general, fence porosity in the range of 0.20-0.50 is considered to give noticeable changes of flow structures behind fences [4] [5] [6].

Physical measurement techniques for investigating the structure of wind flow behind porous fences can be classified into two categories; the Point-Measuring Technique (PMT) and the Whole-Field Measuring Technique (WFMT). Particle-Image Velocimetry (PIV) and Particle-Tracking Velocimetry (PTV) are those WFMT that are non-intrusive to the measuring flow field, with a high spatial resolution and quick response time. However, they are costly and extremely expensive in measuring three dimensional velocity field. Conventional cup type anemometer, Hot-Wire anemometer (HWA), pulsed-Wire anemometer (PWA), Laser-Doppler anemometer (LDA), Phase-Doppler anemometer (PDA), and Ultrasonic anemometer (UA) are PMT measuring sensors. All of these sensors provide time averaged velocity and turbulence intensity values at discrete measuring points. Apart from cup type anemometer, all other PMT techniques mentioned above allow the acquisition of three dimensional wind velocity vectors with a good resolution. HWA and PWA are sensitive to the testing environment, and insensitive to velocity direction and low velocity. LDA and PDA are non-intrusive sensors, with quick response time. Compared to UA, their acquisition and running costs are fairly high. UA is an intrusive measurement sensor, however, it is moderate in cost and easy to operate. Furthermore, it takes measurements at high frequency with a good temporal resolution even in a hostile environment and enables to capture the fluctuations of velocity vectors. These obtained velocity data can be used to calculate velocity magnitudes, turbulence intensity and turbulent kinetic energy. Therefore, as an overall evaluation, UA is an effective physical measuring sensor in investigations of the structure of wind flow around porous fences. However, it is inevitable to mount an UA on a special fixture while taking the measurements. This, together with the structure of the sensor itself will distort the flow field itself, as such, a correction based upon wind tunnel measurements to minimize this intrusive impact is required.

2. Experimental set-up

This work aims to investigate wind flow behavior at the leeward side of different porous fences, through measuring three dimensional velocity vectors at various points along the centerline of the panel, and at different altitudes from the floor of the test section.

The experiments were conducted in an environmental wind tunnel at the Shinjo Cryospheric Environment Laboratory, Japan, which is a closed circuit flow type with a rectangular test section of 1m high, 1m wide and 14m long. It can produce inlet wind velocity from 0m/s to 20m/s. The length of the test section ensures the development of a neutrally stratified boundary layer flow inside the test section. In the present work, the wind tunnel facility was used under ambient conditions to simulate wind blow against a vertical fence at right angles to the wind direction. The wind tunnel is equipped with a state-of-the-art traverse system and control system, which enables measurement at any point along its test section. It is also equipped with a data acquisition system capable of recording all the data including locations of measurement and measurement data.



Fig. 2: The experimental set-up

The physical measurement sensor used in this experiment was a DA-650 (TR-92T) type ultrasonic anemometer manufactured by Kaijo Sonic Corporation in Japan. The Shinjo Cryospheric Environment Laboratory has already evaluated an error correction factor for error resulting from intrusiveness to airflow fields. The sensor is capable of measuring main flow wind velocity in the range of 0-20m/s. The accuracy of operation is within 1% for three dimensional velocity vectors. The resolution is 0.005m/s or less, and the repetition of measurement is 20 times per second.

Outputs corresponding to velocity vectors are in volts, where the longitudinal vector is measured by the voltage of channel 1 multiplied by a factor of 20, while the lateral vector is measured by the voltage of channel 2 multiplied by a factor of 5, and the vertical vector by the voltage of channel 3 multiplied by a factor of 5.

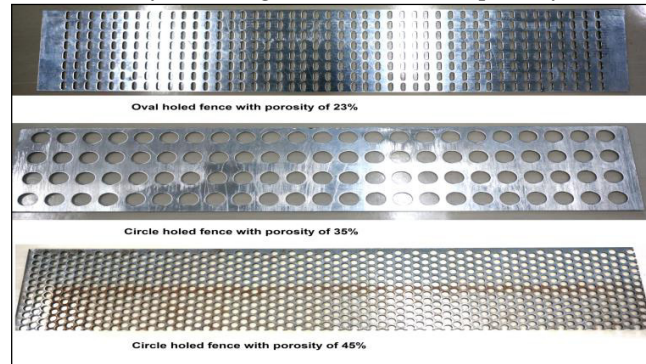


Fig. 3: The testing fence samples

The experimental set-up of the ultrasonic manometer and the porous fence is shown in Fig. 2, while Fig. 3 shows three test samples of porous fences with different porosities.

For the purpose of comparison, identical configuration for all of the samples has been selected, where ($length * height * thickness = 900mm * 150mm * 3mm$). This also ensures a blockage ratio of less than 10% of wind tunnel cross sectional area.

3. Results and discussions

3.1. Visualization of wind flow

Visualization of the wind flow regime for each testing case has been conducted. Moisture was generated by a PIVTEC Aerosol Generator PivPart45-M and was fed through a hole situated in the wind tunnel floor. Under the laser sheet, the motion of moisture behind the fence could be observed, which demonstrated the structure of the wind flow behind the fence.



Fig. 4: Visualization of the fence with 23% porosity

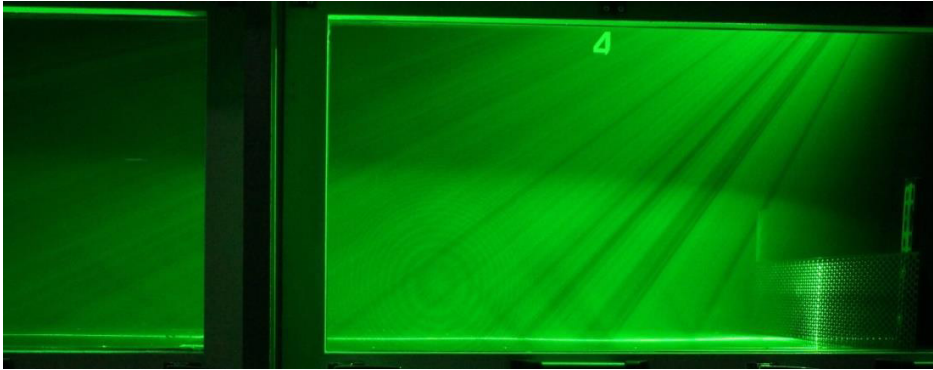


Fig. 5: Visualization of the fence with 35% porosity



Fig. 6: Visualization of the fence with 45% porosity

In the experiments, inlet wind velocity was kept at 10m/s. Three fence samples were prepared with different porosities and geometries, which were 23% oval holed, 35% circle holed and 45% circle holed respectively, visualizations of wind flow around the fences is display in Fig.4-6 respectively.

It can be observed that the fence with 23% porosity demonstrates the strongest recirculating and separated airflow, and reversal flow is clearly observed. The fence with 35% porosity has weak flow separation and reversal flow is hardly observed. The fence with 45% porosity has no flow separation, while reversal flow is observed, which indicates that the flow is dominated by bleed flow at this porosity. The visualization indicates that the impact of porosity on the structure of airflow behind porous fences is significant. It also reveals that there exists a critical porosity, above which the airflow in the leeward side of the fence is dominated by bleed flow and no flow separation occurs under these circumstances. In the present experiment, the critical porosity can be identified just above 35%. At the porosity of 45%, the flow leeward the fence is dominated by bleed flow.

3.2. Structure of turbulence intensity

The ultrasonic anemometer is capable of acquiring 3 dimensional velocity data. During each measurement campaign, wind velocity was measured as a time series of 10 seconds for the three wind vectors (u , v and w), with a time resolution of 100 Hertz. In other words, each wind velocity vector was averaged by 1000 continuous values, these continuous values were regarded as instantaneous data and were saved as DAT file in the computer. Hence, the fluctuation of each wind velocity vector can be obtained from the experiment.

The data were recorded as raw data for each single wind vector on the x -, y -and z - axis (u , v and w) at all measurement positions. Positive u direction of wind vector was defined in the longitudinal direction from upwind to

downwind, positive v direction of wind vector was defined vertically directed from the wind tunnel floor to the top wall, and positive w direction of wind vector was defined laterally directed from right to left.

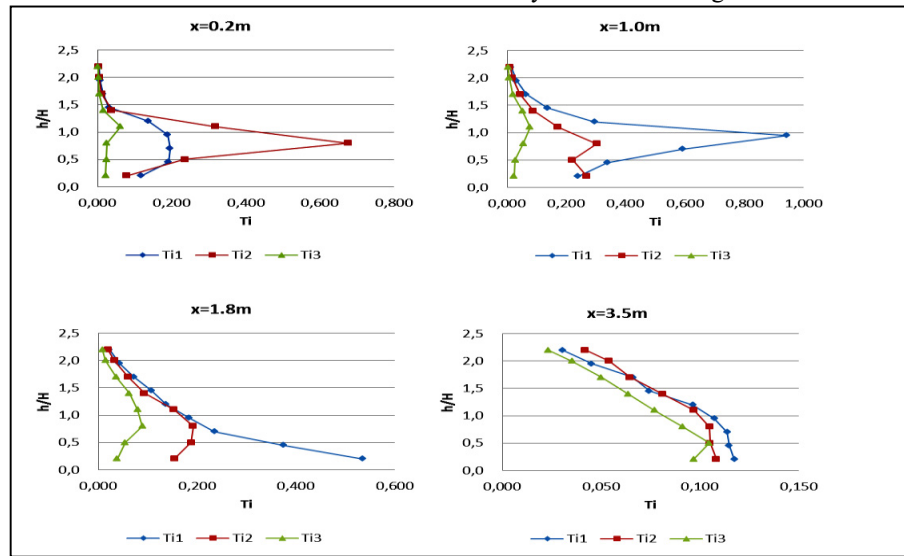


Fig. 7: Vertical turbulence intensities at different longitudinal positions. Ti1 for fence with 23% porosity, Ti2 for fences with 35% porosity, and Ti3 for fence with 45% porosity.

Measurement points along the longitudinal position between the fence and the ultrasonic manometer were taken at 200mm, 600mm, 1000mm, 1400mm, 1800mm, 2600mm, 3500mm, 4500mm and 6000mm. The vertical measuring height was increased in a step height of 50mm from 20mm up to a height of 420mm (from the wind tunnel floor) at each longitudinal measurement point. This set up was designed as such due to the space restrictions of the ultrasonic anemometer and the traverse system. 81 sets of data were yielded for each testing case.

Fig.7 shows the vertical turbulence intensities at different longitudinal positions, where $x=200mm$ in the close fence region, $x=1000mm$ in the wake region, $x=1800mm$ in the internal boundary layer region, and $x=3500mm$ location out of fence effective region. The vertical axis in Fig.7 represents a dimensionless factor which is the ratio between measuring height (h) and fence height (H).

It can be observed from Fig.7 that the fence with 45% porosity created insignificant turbulence in the test domain, and had the lowest level of turbulence intensity among the others. Generally, the fence with 23% porosity produced the highest level of turbulence intensity except at the position of $x=200mm$, which is the close fence region involving bleed flow, shear flow and small vortex stagnation. This complexity can be attributed to fence porosity, however, full understanding of the flow structure in this region has not been achieved so far. In the close fence and wake regions, there was a distinguished peak value at the height from $0.8H$ to $1.0H$ for fences with porosities of 23% and 35%, below which turbulence intensity was observed to increase as the measuring height increased, and above which turbulence intensity was observed to decrease with increasing measuring height. In the internal boundary layer region ($x=1800mm$), only the fence with 23% porosity had a different distribution of turbulence intensity, while for the two other fences, only minor turbulence was observed which can be attributed to their internal boundary layer. In the out of fence effective region (in the regions $h>2H$ or $x>8H$), turbulence intensities for all of the fences under investigation appeared to recover back to the fence free wind flow condition.

Overall, porous fence induced turbulence is sensitive to fence porosity, when the porosity is less than 45%. It was observed that above this porosity the impact on the occurrence of turbulence was insignificant. On the other hand, lower porosity tends to create stronger turbulence and greater turbulent area in the leeward side of the fence.

3.3. Wind velocity reduction

The structure of wind flow through porous fences has been extensively investigated in the physical experiments. It has been widely accepted that porosity in the range from 20% to 50% gives noticeable change of wind velocity structure. Porosity in the range between 20% and 30% is likely to achieve an optimal solution in terms of greater wind reduction and longer shelter distance.

In this paper, correlation between fence effective zone and the reduction rate of wind velocity were under consideration. Fig. 8 shows the effective fence zones assessed by 40% reduction of wind velocity, while Fig. 9 is the effective fence zones assessed by 60% velocity reduction. In the figures, x is the longitudinal distance between the measurement point and the fence. Both X- and Y- Axis are expressed as functions of fence height.

From Fig. 8, it is found that the fence with 45% had the greatest effective zone and the fence with 23% had the smallest, judged under 40% reduction of wind velocity. While from Fig. 9, it is found that the fence with 23% porosity created the greatest effective fence zone and the fence with 45% produced the smallest, judged under 60% reduction of wind velocity. It also can be observed that the longitudinal effective shelter distance tends to increase with increasing fence porosity. In the region $x < 13H$, the fence with 23% porosity displayed best performance.

Results of this work reveal that the optimal design of porous fence should take into consideration the targeted reduction rate of wind velocity.

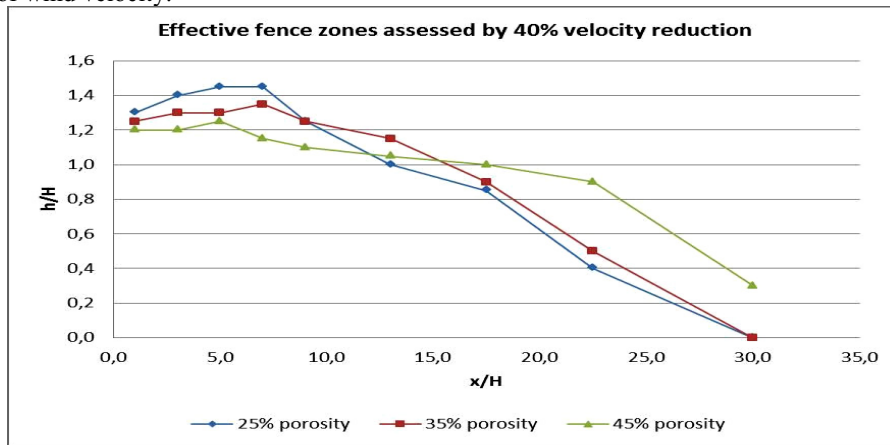


Fig. 8: The effective fence zones assessed by 40% velocity reduction

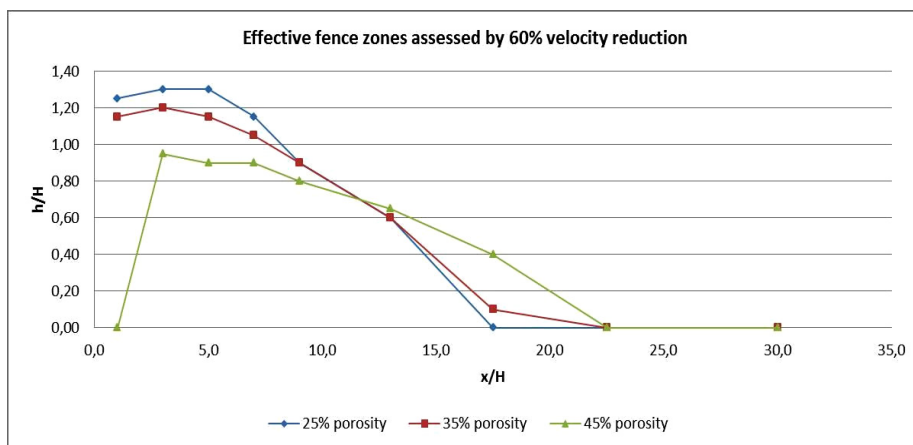


Fig.9: The effective fence zones assessed by 60% velocity reduction

4. Conclusions

Through analysis of experiment results it was found that porosity has profound influence on the structure of leeward wind flow velocity and turbulence. Being the most important structural feature in the porous fence design, optimizing porosity of fence will offer the fence with optimal protection at the minimum cost. The optimal design also needs to take into consideration the targeted reduction rate of wind velocity. Neither the distribution of wind velocities nor the structure of turbulence alone can provide sufficient information to assess the performance of porous fences.

It is concluded that the ultrasonic anemometer is able to capture the fluctuations of three dimensional velocity vectors. The acquired data were used to describe the structures of wind velocity and turbulence leeward of a heathy shape. However, both of the ultrasonic anemometer and the traverse intruded in the flow regime, which raises great concerns about the accuracy of measurements. Further work is needed to evaluate such error by concomitant methods through comparison to no-intrusive equipment, such as Particle Image Velocimetry and Particle Image Tracking equipment.

5. Acknowledgements

This work is financed by the Norwegian Research Council under project number (ColdTech) 195153. The authors would also like to thank the National Research Institute for Earth Science and Disaster Prevention in Japan for providing the facilities at Shinjo Cryospheric Environment Laboratory, Snow and Ice Research Centre and would like to acknowledge the contribution of the industrial partner in this project: IKM dsc AS, Norway.

References

- [1] Yizhong Xu and Mohamad Y. Mustafa, "Investigation of the Structure of Airflow behind a Porous Fence Aided by CFD Based Virtual Sensor Data," *Sensors & Transducers*, Vol. 185, Issue 2, February 2015, pp. 149-155.
- [2] Brandle, James R. and Finch, Sherman, EC91-1763-B How Windbreaks Work, Historical Materials from University of Nebraska-Lincoln Extension. Paper 4709., 1991.
- [3] Z. Dong, W. Luo, G. Qian, P. Lu and H. Wang, "A wind tunnel simulation of the mean velocity field behind upright porous wind fences," *Agricultural and Forest Meteorology*, vol. 146, no. 1, pp. 82-93, 2007.
- [4] M. Jensen, Shelter effect: investigations into Aerodynamics of shelter and its effects on climate and crops, Copenhagen: Danish Tech. Press, 1954.
- [5] N. Tani, On the wind tunnel test of the model shelter hedge," in , 1958., *Bulletin of the Natinal Institute for Agricultural Sciences*, 1958.
- [6] J. Raine and D. Stevenson, "Wind protection by model fences in simulated atmospheric boundary layer," *Industrial Aerodynamics*, vol. 2, no. 1, pp. 159-180, 1977.
- [7] L. Hagen, t. J., and E. L. Skidmore, "Turbulent velocity fluctuations and vertical flow as affected by windbreak porosity," *Trans. ASAE* , vol. 14, no. 4, pp. 634-637, 1971.